Available online at www.sciencedirect.com
SCIENCE DIRECT®
Biochemical and Biophysical Research Communications 322 (2004) 326–332
BBRC
www.elsevier.com/locate/ybbrc

Interaction between the internal motif KTXXXI of Idax and mDvl PDZ domain

Timothy B.C. London[a], Ho-Jin Lee[a], Youming Shao[a], Jie Zheng[a,b,*]

[a] Department of Structural Biology, St. Jude Children's Research Hospital, Memphis, TN 38105, USA
[b] Department of Molecular Sciences, University of Tennessee Health Science Center, Memphis, TN 38163, USA

Received 13 July 2004

Abstract

Dishevelled (Dvl) is the essential signal transduction component of both canonical and non-canonical Wnt signaling pathways. The cysteine-rich protein Idax acts as a negative regulator of Wnt signaling in mammals by interaction with Dvl in the region of the PDZ domain. In an effort to clarify the structural basis of this interaction, we used nuclear magnetic resonance spectroscopy to study the interaction of the Dvl PDZ domain with Idax. We first confirmed that the C-terminal region of Idax consisting of residues 109–198 binds to the PDZ domain of mouse Dvl-1 at the conventional C-terminal peptide-binding groove. However, instead of the C-terminus of Idax, we showed that a peptide of an internal sequence of Idax containing a KTXXXI motif is important in the interaction with a binding affinity estimated at 56 μM. Such internal motif identified in this study suggests a new type of sequence motif recognition for Dvl PDZ domain.

Keywords: Wnt signaling; Idax; Binding motif; PDZ domain; NMR; Protein–ligand interaction; Protein structure

The Wnt family of extracellular signaling proteins plays a crucial role in the developmental processes of metazoan animals [1,2]. In vertebrates, Wnt signaling controls cell fate and specification in developmental processes which include organ development, axis formation, limb development, and gastrulation [3,4]. Aberrant Wnt signaling is found in a range of tumor types and notably in about 80% of colorectal cancers [5–8]. The Wnt signaling pathway has also been implicated in Alzheimer's disease [9].

In the mammalian canonical β-catenin branch of the Wnt signaling pathway, interaction of Wnt with the Frizzled (Fz) receptor enhances the ability of the cytoplasmic Dishevlled (Dvl) protein to inhibit the activity of glycogen synthase kinase 3β (GSK-3β) [1]. GSK-3β exists in the cytoplasm in complex with the scaffold protein Axin and tumor suppressor protein adenomatous polyposis coli (APC) [10] and functions to phosphorylate β-catenin thereby marking it for ubiquitinylation and subsequent degradation. Wnt signaling causes cytosolic β-catenin levels to increase allowing translocation to the nucleus resulting in transcription of the target genes which include *c-myc*, *fra*, *jun*, and *cyclin D1* [11,12]. In *Drosophilia* and *Xenopus*, there is a non-canonical branch of Wnt signaling pathway which diverges from the β-catenin branch at the level of Dsh or Xdsh (the respective Dvl homologues in these species) and specifies planar polarity [13]. The molecular mechanism by which Dsh/Dvl distinguishes signals from a common upstream receptor and activates these divergent signaling pathways is as yet unclear.

Dvl proteins are ~750 aa in size and characterized by three highly conserved domains; an N-terminal DIX (Dishevelled–Axin) domain, a central PDZ (Post Synaptic Density-95, Discs Large and Zonula

* Corresponding author. Fax: +1 901 495 3032.
E-mail address: Jie.Zheng@stjude.org (J. Zheng).

0006-291X/$ - see front matter © 2004 Elsevier Inc. All rights reserved.
doi:10.1016/j.bbrc.2004.07.113

Occludens-1) domain, and a C-terminal DEP (Dishevelled-EGL-10-Pleckstrin) domain [14,15]. The central conserved PDZ domain of Dvl is ~90 amino acids in size and has a role, if somewhat unclear, in both the PCP and β-catenin branches of the Wnt signaling pathway [13]. Several of the many Dsh/Dvl Associated Proteins (DAPs) that modify Wnt signaling at the level of Dsh/Dvl bind to Dvl fragments that include the PDZ domain [16–20]. However, interpretation of these results is made difficult by the fact that some of the constructs contain an adjacent basic region with putatively phosphorylated residues whereas others do not [20]. Moreover, these studies give no insight into the mechanism of binding. The specific mechanisms of binding of the Dvl PDZ domain to DAPs have relevance in the search for targeted cancer therapies as certain DAPs have been shown to have an inhibitory effect on the Wnt signaling pathway. One of these proteins is Idax (for Inhibitor of the Dvl and Axin complex).

Idax was isolated as a Dvl-1 PDZ-binding protein in yeast two-hybrid screens of rat brain cDNA [16]. Rat Idax (rIdax) encodes a 198 amino acid cysteine-rich protein, which has been shown to antagonize Wnt/β-catenin signaling when levels are increased in tissue culture cells. The rIdax shows 100% identity to mouse and human Idax (mIdax and hIdax) and 83% identity to *Xenopus* Idax (xIdax) (Fig. 1). BLAST analysis has revealed additional Idax-related sequences in invertebrate and vertebrate genomes [16]. Although it has been established that there is a biologically significant interaction between rIdax and the PDZ domain of Dvl-1, the structural mechanism of its binding is as yet undefined [16]. In this study we used nuclear magnetic resonance spectroscopy (NMR) to investigate the interaction of the PDZ domain (residues 251–342) of mouse Dvl-1 (mDvl-1) with rat Idax (rIdax). By use of peptides corresponding to short stretches of the Idax, the amino acid sequence motif important to binding was characterized. This study will be useful to understand the Wnt signaling pathway and to identify the PDZ-binding motif of the other Dsh/Dvl associated proteins.

Materials and methods

Production of ^{15}N-labeled mDvl-1 PDZ domain. The PDZ construct used represented a 94 amino acid fragment of the mouse Dvl-1 protein starting from residue 244 and extending to residue 341 of the overall protein as described before [15]. The transformed cells were grown 1 L MOPS cultures containing $^{15}NH_4Cl$ as the sole source of nitrogen at 37 °C with shaking at 225 rpm until the absorbance at 600 nm reached ~0.7. Protein expression was chemically induced by the addition of isopropyl-1-thio-β-D-galactoside (IPTG) to a final concentration of 1 mM and the cells were harvested 6 h later by centrifugation.

Production of unlabeled rat Idax. The Idax construct used was the C-terminal half of the protein running from residue 109 to the C-terminus. This was subcloned into pET28b (Novagen) and transformed into *Escherichia coli* strain BL21(DE3)-RP. The transformed cells were grown in 1 L LB cultures at 37 °C with shaking at 225 rpm until absorbance of the cells at 600 nm reached ~0.7. Protein expression was chemically induced with 1 mM IPTG and approximately 4 h later the cells were harvested by centrifugation.

Purification procedure. The cell pellets were resuspended in lysis buffer (20 mM phosphate, 150 mM NaCl, and 1 mM EDTA, pH 7.8) containing a cocktail of protease inhibitors and lysed by mechanical lysis using a French press. The cell lysate was separated by centrifugation and Promega Ni–NTA beads were added to the supernatant and incubated overnight at 4 °C with rocking. After incubation the beads were pelleted out of the supernatant by centrifugation. The beads were then transferred to a column and washed with wash buffer (20 mM phosphate, 150 mM NaCl, and 1 mM EDTA, pH 7.8) containing 50 mM imidazole. The His-tagged protein was eluted off the beads with 200 and 500 mM imidazole containing wash buffer and collected in 15 ml fractions. The protein containing fractions were dialyzed into 100 mM phosphate, 100 mM NaCl, 1 mM EDTA, and 2 mM DTT (pH 7.8) before being further purified by fast performance liquid chromatography (FPLC) in a Superdex 75-pg column (Amersham Pharmacia) at 4 °C. Centrifugal spin concentrators (Vivascience) were used to concentrate the protein before NMR.

Peptide synthesis and purification. A number of short synthetic peptides were designed including putative-binding motifs based on our previous work. Acetyl groups were attached to the N-terminus of each peptide and amino groups attached to the C-terminus. The peptides were synthesized by the Hartwell Center for Bioinformatics and Biotechnology at St. Jude Children's Research Hospital and purified by reverse-phase high performance liquid chromatograph.

NMR spectroscopy. NMR experiments were performed at 25 °C using a Varian INOVA 600-MHz spectrometer. Samples consisted of the PDZ domain (0.5–1 mM) in 100 mM phosphate (pH 7.5), 100 mM NaCl, 1 mM EDTA, and 2 mM DTT with the addition of Idax or peptides. ^{15}N-HSQC experiments were performed to detect chemical shift perturbation in the spectra of PDZ indicative of binding. NMR spectra were processed using NMRpipe [21] software and analyzed by SPARKY [22].

Curve fitting for determination of binding affinity using NMR. ^{15}N and ^{1}H chemical shift values for the moving peaks in the titration experiment were determined in SPARKY for each of the successive titration points. The averaged chemical shift change for the moving peaks was calculated by subtracting the reference spectrum (the free protein spectrum) from chemical shift values of the titration points and then averaging the ^{15}N and ^{1}H values using Eq. (1) [23].

$$\Delta\delta_{\text{avg}} = \sqrt{\frac{(\Delta\delta\text{N}/5)^2 + \Delta\delta\text{H}^2}{2}}, \tag{1}$$

$\Delta\delta$N is the chemical shift change of the amide nitrogen and $\Delta\delta$H is the chemical shift change of the amide proton [23–25]. The division of the amide chemical shift by 5 accounts for the difference in chemical shift scales of the nitrogen and proton dimensions.

The averaged chemical shift change was plotted against the molar ratio of the peptide to the PDZ domain. A two-parameter nonlinear least squares regression curve fitting was performed in Origin version 6.1 (Microcal Software, Northampton, MA) using a one-site binding model which corrects for the dilution effect of adding the ligand to the protein.

$$\Delta\delta_{\text{binding}} = \frac{1}{2}\Delta\delta_{\max}\left(A - \sqrt{A^2 - 4R}\right),$$
$$A = 1 + R + \frac{PR + C}{PCK_{\text{a}}}. \tag{2}$$

In this equation R is the [KTXXXI]:[^{15}N-PDZ] ratio, $\Delta\delta_{\text{binding}}$ is the chemical shift change relative to the free protein when titrating the ligand, $\Delta\delta_{\max}$ is the chemical shift change for $R \to \infty$, P is the concentration of ^{15}N-PDZ at the beginning of the titration, C is the stock KTXXXI peptide solution concentration, and K_{a} is the association constant [23].

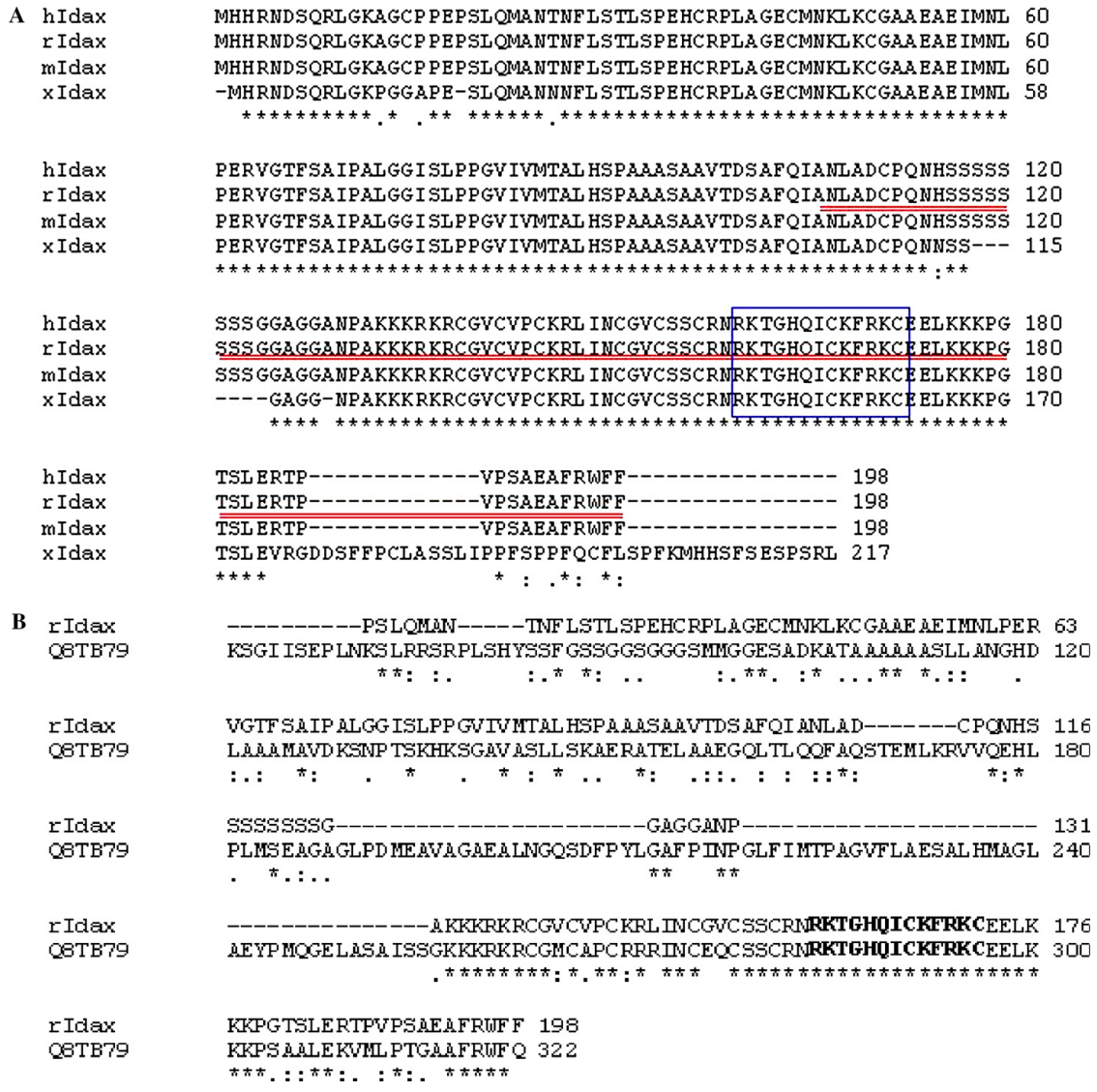

Fig. 1. Amino acid sequential alignments (A) of hIdax, rIdax, mIdax, and xIdax, (B) and of rIdax and a putative MAPK or NF-κB-binding protein (Q8TB79) by using Cluster W. Dashes show a gap by alignment. The red line shows the construct of Idax (109–198) that we made. The blue box is the minimum region of Idax that is necessary for binding to Dvl PDZ domain. (*) indicates that residues are identical in the alignment; (:) indicates that conserved substitutions have been observed; and (.) indicates that semi-conserved substitutions are observed.

Fluorescence spectroscopy. A Jobin-Yvon Fluorolog-3 spectrofluorometer (Jobin-Yvon) was used to obtain the fluorescence measurements of the interaction between the PDZ domain of mDvl1 and the rIdax peptide. Titration experiments were performed at 25 °C in a phosphate buffer (0.1 M potassium phosphate; 0.5 mM EDTA, pH 7.5). The peptide ligand (2.1 mM) was injected into the 2.0-mL sample cell that contained either the PDZ domain (25 μM). The excitation wavelength was 290 nm (slit width, 5 nm), and the fluorescence emissions from 320 to 370 nm (slit width, 5 nm) were recorded (Fig. 4A) during the titration of rIdax peptide, whose concentrations ranged from 2 to 90 μM. The fluorescence data were analyzed by using the ORIGIN program (Microcal). The K_D value was calculated from a reciprocal plot of fluorescence intensity quenching (ΔF) against the concentration of the rIdax peptide for two sets of titration data (Eq. (3))

$$\frac{1}{\Delta F} = \frac{1}{F_{max}} + \frac{K_D}{F_{max}} \cdot \frac{1}{[S]}, \quad (3)$$

ΔF is the change of fluorescence intensity and [S] is the solute concentration.

Results and discussion

The C-terminal half of the rIdax protein is necessary for both association with Dvl and inhibition of canonical Wnt signaling, the minimal region of rIdax required for binding to Dvl remains to be clarified [16]. Thus, we first made the rIdax (109–198) construct representing its C-terminal half from residue 109 to 198 as shown in Fig. 1A. Although it is reported that rIdax (109–198) interacts biologically with the Dvl1 PDZ domain, we confirmed this interaction with NMR spectroscopy at the atomic level.

Fig. 2A shows the ^{15}N-HSQC spectra of mDvl PDZ in the presence of rIdax (109–198) at the 1:1 concentration. The interaction between the PDZ domain and rIdax (109–198) could be analyzed by comparison of ^{15}N-HSQC spectra between a reference spectrum of the

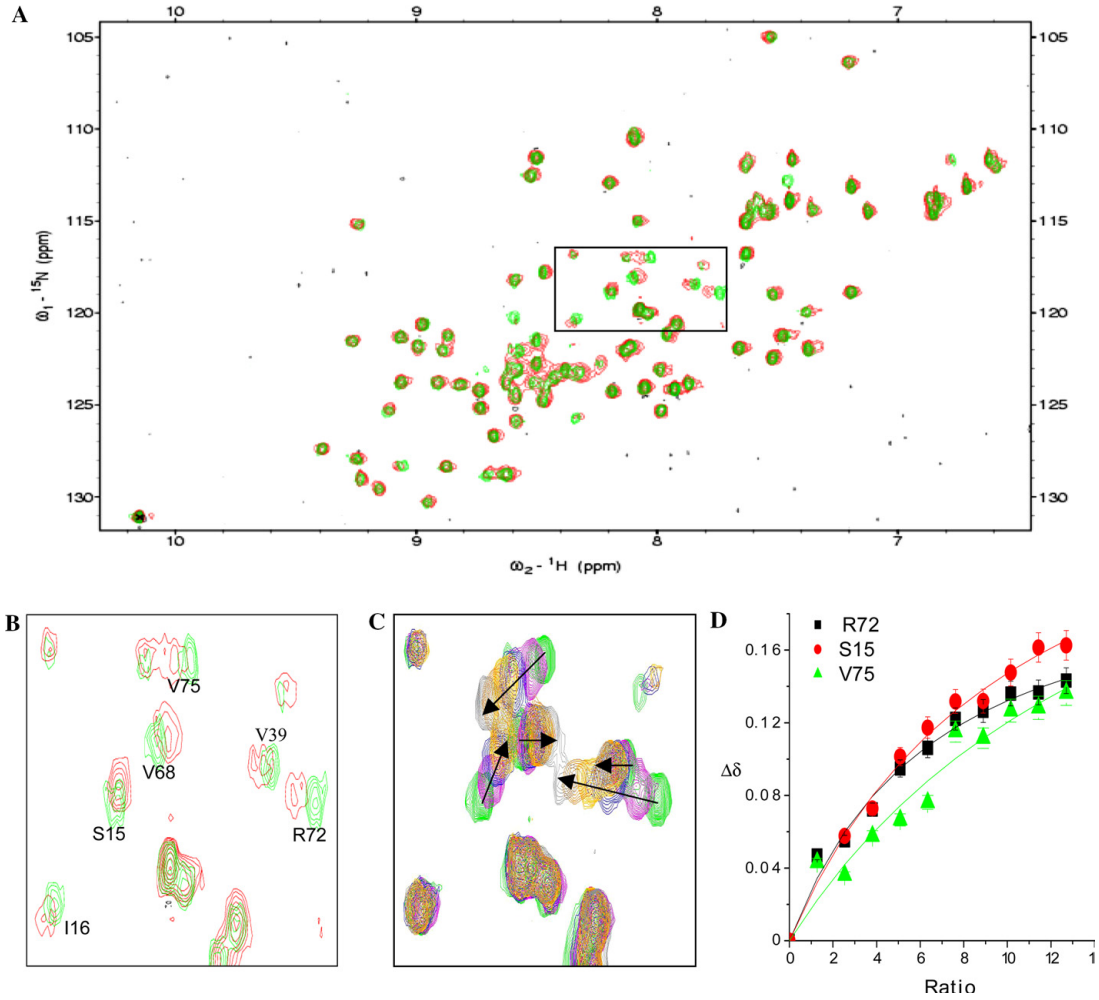

Fig. 2. The C-terminal half of rIdax directly binds to mDvl1 PDZ domain. (A) ^{15}N-HSQC of the mDvl1 PDZ domain alone (green) with Idax (109–198) (red) in 1:1 molar ratio at pH 7.8 and 25 °C. (B) The enlarged spectrum of 1:1 PDZ:rIdax (109–198) complex is corresponding to the residues of the α-helix B and β-sheet B regions in the PDZ domain. (C) Peptide-binding ^{15}N-HSQC spectrum of mDvl1 PDZ during the titration, showing the similar change of chemical shift as protein-binding HSQC spectrum. (D) The averaged chemical shift change was plotted against the molar ratio of the peptide to the PDZ domain.

ligand-free protein and a similar spectrum acquired in the presence of ligand. Information on binding can be obtained from the chemical shift change between the two spectra [25]. Fig. 2B is the enlarged spectrum of 1:1 PDZ:rIdax (109–198) protein which represents the amino acid residues of PDZ-binding site, showing the interaction between two proteins. Based on resonance assignment of ^{15}N-PDZ domain of mDvl-1, we found that the rIdax (109–198) protein bound at the same site as Frizzled peptide on the C-terminal peptide-binding groove between α-helix B and β-sheet B (Fig. 3A) of PDZ domain comprising six β stands (βA to βF) and two α-helices (αA and αB) [15]. Connolly surface plotting based on the lyphophilic potential of the amino acids (Fig. 3B) reveals that the peptide-binding groove is situated in a hydrophobic pocket.

Idax does not contain the canonical C-terminal PDZ domain-binding motif (S/TXV) found in other PDZ-binding proteins. Also, the C-terminal amino acids of Idax are not conserved in all species, e.g., xIdax (Fig. 1A). This suggests that the C-terminal amino acids are not important to the interaction with the PDZ domain. Because the PDZ-binding site of rIdax (109–198) is same with that of Frizzled, we reasoned that an internal sequence of rIdax (109–198) protein would be involved in this interaction. Previously, we found that the conserved **KTXXXW** internal sequence of Frizzled associates with the mDvl-1 PDZ domain [15]. Based on this finding, we designed peptide that has a similar mDvl1 PDZ-binding motif, which has a **KTXXXI** motif (Ac-R**KT**GHQ**I**CKFRKC-NH_2) (see Fig. 1A, blue box). To verify whether this peptide binds the mDvl-1 PDZ domain, we obtained the ^{15}N-HSQC spectra of the PDZ domain during the titration of the rIdax peptide as a function of concentration (Fig. 2C). As shown in Fig. 2C, the chemical shift changes of peptide-binding ^{15}N-HSQC spectra are similar to that of rIdax (109–198) protein-binding one (Fig. 2B). This indicates that

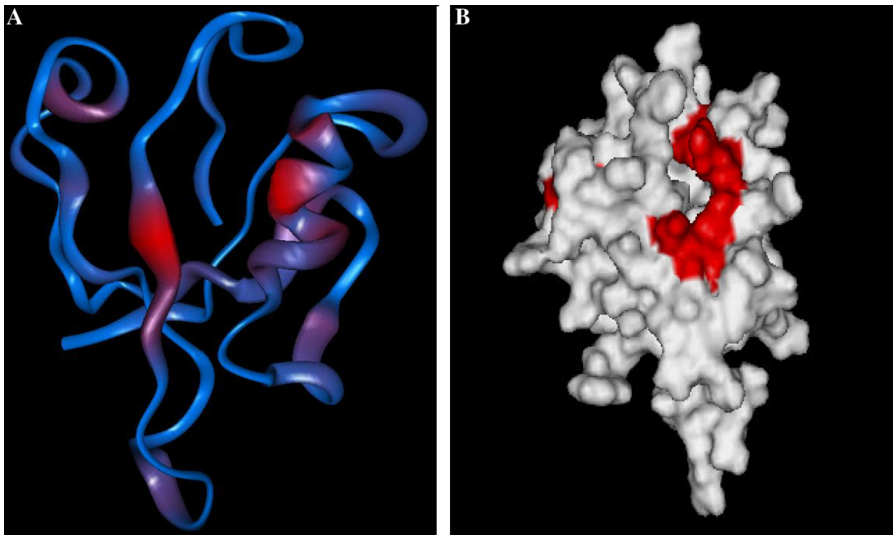

Fig. 3. The binding site of PDZ is located at the α-helix B and β-sheet B regions. (A) A ribbon representation of the backbone of structure of the PDZ domain. The thickness and color of the ribbon is proportional to the weighted sum (in ppm) of the proton and amide chemical shifts upon binding of Idax (red, high; blue, low) (B) a Connolly rendered surface representation of the mDvl-1 PDZ domain. Residues for which the weighted sum of the chemical shift values was greater than 0.01 on binding of Idax are marked in red.

rIdax peptide indeed associates with the mDvl-1 PDZ domain such as the rIdax (109–198) protein, implying that a KTXXXI motif of rIdax peptide is a minimum region required for PDZ binding.

To obtain an insight into the binding event between the mDvl-1 and rIdax protein, we obtained the binding affinity (K_D) between PDZ and rIdax peptide by using NMR spectroscopy. By plotting of the averaged chemical shift change ($\Delta\delta_{avg}$) against the molar ratio of the peptide to the PDZ domain, the K_D value of about 5 mM was obtained (Fig. 2D) [23]. Since the K_D value for (calculated by the same method as in this study) Fz7 interaction with the PDZ domain of mDvl1 was 1 mM, the low K_D value for rIdax peptide suggests that Idax would not be an effective inhibitor.

Although NMR is useful for the study of weak protein–protein interactions in solution, it is not the best method for calculating dissociation constants due to the high interference of removing the protein solution from the NMR tube each time the peptide is added and replacing it. Thus, dissociation constants calculated by this method can only be treated as the upper limit for the interactions [26]. Therefore, we used another method to obtain the binding affinity of rIdax peptide and mDvl1 PDZ domain; by measuring the fluorescence of PDZ domain. The binding of rIdax peptide quenched the intrinsic tryptophan fluorescence of the Dvl PDZ domain as a function of concentration (Fig. 4A). By monitoring such changes in fluorescence intensity, we determined the binding affinity between the rIdax

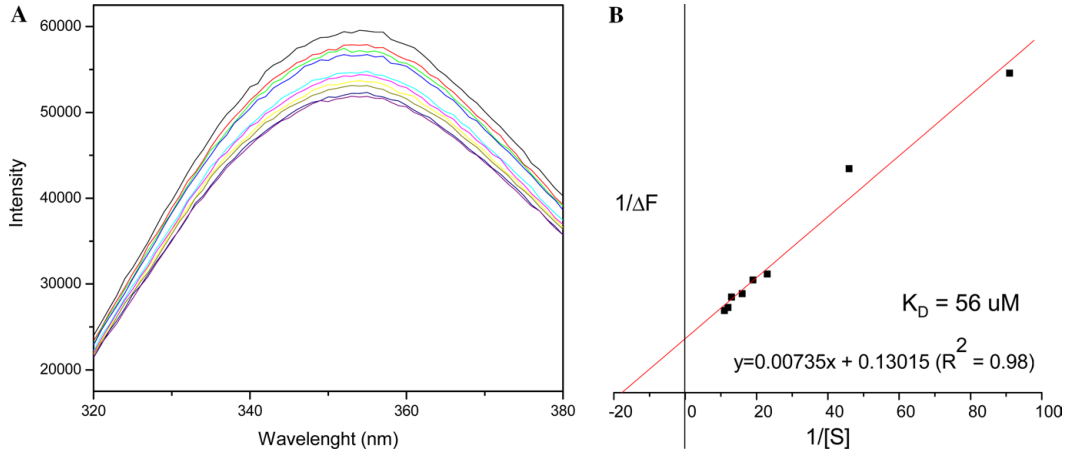

Fig. 4. (A) Fluoresce spectra of mDvl1 PDZ domain during the titration of the peptide. The binding of the peptide quenched the intrinsic tryptophan fluorescence of the PDZ domain. (B) The binding affinity between PDZ and Idax peptide was determined from a reciprocal plot of fluorescence intensity quenching (ΔF) against the concentration of the Idax peptide.

peptide and the PDZ domain that was 56 μM (Fig. 4B). Compared with the binding affinity of PDZ domain for the Dpr/Frodo or Fz7 peptide obtained before [15], the rIdax peptide weakly binds to the PDZ domain, however, we expect that this interaction would be sufficient to disturb the PDZ-related interaction.

Given that rIdax appears to bind at the same site on the PDZ domain of Dvl-1 as the cell surface receptor that activates it, the question is raised as to how binding of Fz results in the signaling being relayed downstream and binding of Idax results in inhibition of Wnt signaling. It is possible that in vivo, Idax acts as a competitive inhibitor, blocking the interaction between Fz7 and the PDZ-binding site of Dvl, and then inhibiting Wnt signaling. The other explanation is also possible. Because several proteins such as CKIε, AXIN, and Nkd also associate with the Dvl protein [18,20,27,28], these proteins may bind to the same site on the PDZ domain. Thus, an alternative hypothesis is that different binding affinities of these proteins and Dvl PDZ domain are related to the resultant up- or downregulatory effect on Wnt signaling.

In these experiments the minimal region of Idax required for binding to the mDvl PDZ domain was identified to be a short peptide containing a KTXXXI motif. This is consistent with our previous work in which a peptide containing a conserved KTXXXW motif of the Frizzled receptor bound to mDvl-1 PDZ at same site [15]. The results suggest that the hydrophobic properties of the final amino acid in the motif are important to binding rather than the exact residue. Thus, the motif may in fact be KTXXXΦ (where Φ is any hydrophobic residue), implying that several of the many Dsh/Dvl associated proteins (DAPs) also have a similar binding motif.

A Blast program search of the full length Idax amino acid sequence revealed that the C-terminal region shares homology with a putative MAPK (mitogen-activated protein kinase) activating protein and NF-κB activating protein (Q8TB79) with the region of exact homology being centered around the KTXXXI motif (Fig. 1B) [29]. This implies that these proteins may be able to bind to the PDZ domain of mDvl-1 and shows possible cross talk between the Wnt signaling pathway and these other major pathways mediated through the PDZ domain of mDvl. Our collaborator is examining a possibility of the cross talk between two pathways. Recently, Michiue et al. [30] suggested that the C-terminal half of xIdax was homologous with the CXXC-zinc finger motif including two leukemia-associated genes, LCX and MLL. The results imply that Idax proteins may play several roles in signaling pathways.

In summary, we identified and characterized the protein–protein interaction between rIdax and Dvl PDZ domain by using NMR spectroscopy. The PDZ-binding site of rIdax (109–198) is the conventional C-terminal grove region. Given that the KTXXXW motif of Frizzled directly binds to Dvl PDZ domain, we could identify the minimum region of rIdax that is necessary for binding. This was verified with NMR and fluorescence spectroscopy. Although several Dsh/Dvl, especially PDZ domain, associated proteins have been identified, the essential region required for binding remains unknown. The KTXXXI motif identified in this paper represents novel internal PDZ-binding motif. Coupled with the KTXXXW motif identified for the Frizzled receptor [15], the motif KTXXX(hydrophobic,Φ) could represent a new type of PDZ ligand. Thus, this study could be helpful to identify the PDZ-binding motif of Dsh/Dvl associated proteins and to understand the Wnt signaling pathway in more detail.

Acknowledgments

This work was supported by National Institutes of Health Grant GM61739 and the American Lebanese Syrian Associated Charities. We thank Professor Akira Kikuchi for kindly providing the cDNA constructs of Idax and Dr. Weixing Zhang for technical support. Timothy B.C. London is a student in the Department of Biology and Biochemistry, University of Bath, Bath BA2 7AY, United Kingdom.

References

[1] K.M. Cadigan, R. Nusse, Wnt signaling: a common theme in animal development, Genes Dev. 11 (1997) 3286–3305.
[2] A. Wodarz, R. Nusse, Mechanisms of Wnt signaling in development, Annu. Rev. Cell Dev. Biol. 14 (1998) 59–88.
[3] T.C. Dale, Signal transduction by the Wnt family of ligands, Biochem. J. 329 (Pt 2) (1998) 209–223.
[4] J.R. Miller, A.M. Hocking, J.D. Brown, R.T. Moon, Mechanism and function of signal transduction by the Wnt/beta-catenin and Wnt/Ca^{2+} pathways, Oncogene 18 (1999) 7860–7872.
[5] B. Lustig, J. Behrens, The Wnt signaling pathway and its role in tumor development, J. Cancer Res. Clin. Oncol. 129 (2003) 199–221.
[6] M. Peifer, P. Polakis, Wnt signaling in oncogenesis and embryogenesis—a look outside the nucleus, Science 287 (2000) 1606–1609.
[7] M.J. Smalley, T.C. Dale, Wnt signalling in mammalian development and cancer, Cancer Metastasis Rev. 18 (1999) 215–230.
[8] F.T. Kolligs, G. Bommer, B. Goke, Wnt/beta-catenin/tcf signaling: a critical pathway in gastrointestinal tumorigenesis, Digestion 66 (2002) 131–144.
[9] G.V.De Ferrari, N.C. Inestrosa, Wnt signaling function in Alzheimer's disease, Brain Res. Brain Res. Rev. 33 (2000) 1–12.
[10] S. Kishida, H. Yamamoto, S. Ikeda, M. Kishida, I. Sakamoto, S. Koyama, A. Kikuchi, Axin, a negative regulator of the wnt signaling pathway, directly interacts with adenomatous polyposis coli and regulates the stabilization of beta-catenin, J. Biol. Chem. 273 (1998) 10823–10826.
[11] B. Mann, M. Gelos, A. Siedow, M.L. Hanski, A. Gratchev, M. Ilyas, W.F. Bodmer, M.P. Moyer, E.O. Riecken, H.J. Buhr, C. Hanski, Target genes of beta-catenin-T cell-factor/lymphoid-enhancer-factor signaling in human colorectal carcinomas, Proc. Natl. Acad. Sci. USA 96 (1999) 1603–1608.

[12] M. Shtutman, J. Zhurinsky, I. Simcha, C. Albanese, M. D'Amico, R. Pestell, A. Ben Ze'ev, The cyclin D1 gene is a target of the beta-catenin/LEF-1 pathway, Proc. Natl. Acad. Sci. USA 96 (1999) 5522–5527.
[13] M. Boutros, M. Mlodzik, Dishevelled: at the crossroads of divergent intracellular signaling pathways, Mech. Dev. 83 (1999) 27–37.
[14] H.C. Wong, J. Mao, J.T. Nguyen, S. Srinivas, W. Zhang, B. Liu, L. Li, D. Wu, J. Zheng, Structural basis of the recognition of the dishevelled DEP domain in the Wnt signaling pathway, Nat. Struct. Biol. 7 (2000) 1178–1184.
[15] H.C. Wong, A. Bourdelas, A. Krauss, H.J. Lee, Y. Shao, D. Wu, M. Mlodzik, D.L. Shi, J. Zheng, Direct binding of the PDZ domain of Dishevelled to a conserved internal sequence in the C-terminal region of Frizzled, Mol. Cell 12 (2003) 1251–1260.
[16] S. Hino, S. Kishida, T. Michiue, A. Fukui, I. Sakamoto, S. Takada, M. Asashima, A. Kikuchi, Inhibition of the Wnt signaling pathway by Idax, a novel Dvl-binding protein, Mol. Cell. Biol. 21 (2001) 330–342.
[17] M. Park, R.T. Moon, The planar cell-polarity gene stbm regulates cell behaviour and cell fate in vertebrate embryos, Nat. Cell Biol. 4 (2002) 20–25.
[18] R. Rousset, J.A. Mack, K.A. Wharton Jr., J.D. Axelrod, K.M. Cadigan, M.P. Fish, R. Nusse, M.P. Scott, Naked cuticle targets dishevelled to antagonize Wnt signal transduction, Genes Dev. 15 (2001) 658–671.
[19] D. Yan, J.B. Wallingford, T.Q. Sun, A.M. Nelson, C. Sakanaka, C. Reinhard, R.M. Harland, W.J. Fantl, L.T. Williams, Cell autonomous regulation of multiple Dishevelled-dependent pathways by mammalian Nkd, Proc. Natl. Acad. Sci. USA 98 (2001) 3802–3807.
[20] K.A. Wharton Jr., Runnin' with the Dvl: proteins that associate with Dsh/Dvl and their significance to Wnt signal transduction, Dev. Biol. 253 (2003) 1–17.
[21] F. Delaglio, S. Grzesiek, G.W. Vuister, G. Zhu, J. Pfeifer, A. Bax, NMRPipe: a multidimensional spectral processing system based on UNIX pipes, J. Biomol. NMR 6 (1995) 277–293.
[22] T.D. Goddard, D.G. Kneller, SPARKY 3. (3.106), 2002, University of California, San Francisco.
[23] J.A. Worrall, W. Reinle, R. Bernhardt, M. Ubbink, Transient protein interactions studied by NMR spectroscopy: the case of cytochrome C and adrenodoxin, Biochemistry 42 (2003) 7068–7076.
[24] D.S. Garrett, Y.J. Seok, A. Peterkofsky, G.M. Clore, A.M. Gronenborn, Identification by NMR of the binding surface for the histidine-containing phosphocarrier protein HPr on the N-terminal domain of enzyme I of the *Escherichia coli* phosphotransferase system, Biochemistry 36 (1997) 4393–4398.
[25] S.W. Homans, NMR spectroscopy tools for structure-aided drug design, Angew. Chem. Int. Ed. Engl. 43 (2004) 290–300.
[26] J. Zheng, S.M. Cahill, M.A. Lemmon, D. Fushman, J. Schlessinger, D. Cowburn, Identification of the binding site for acidic phospholipids on the pH domain of dynamin: implications for stimulation of GTPase activity, J. Mol. Biol. 255 (1996) 14–21.
[27] S. Hino, T. Michiue, M. Asashima, A. Kikuchi, Casein kinase I epsilon enhances the binding of Dvl-1 to Frat-1 and is essential for Wnt-3a-induced accumulation of beta-catenin, J. Biol. Chem. 278 (2003) 14066–14073.
[28] W. Luo, S.C. Lin, Axin: a master scaffold for multiple signaling pathways, Neurosignals 13 (2004) 99–113.
[29] A. Matsuda, Y. Suzuki, G. Honda, S. Muramatsu, O. Matsuzaki, Y. Nagano, T. Doi, K. Shimotohno, T. Harada, E. Nishida, H. Hayashi, S. Sugano, Large-scale identification and characterization of human genes that activate NF-kappaB and MAPK signaling pathways, Oncogene 22 (2003) 3307–3318.
[30] T. Michiue, A. Fukui, A. Yukita, K. Sakurai, H. Danno, A. Kikuchi, M. Asashima, XIdax, an inhibitor of the canonical Wnt pathway, is required for anterior neural structure formation in *Xenopus*, Dev. Dyn. 230 (2004) 79–90.